Hysteresis loop and torque experiments on a random anisotropy system

B. Dieny, B. Barbara, G. Fillion, M. Maeder, B. Michelutti

J. Physique **48** (1987) 1741-1749 OCTOBRE **1987**, PAGE 1741

Classification
Physics Abstracts
75.50 — 75.60

Hysteresis loop and torque experiments on a random anisotropy system

B. Dieny, B. Barbara, G. Fillion, M. Maeder and B. Michelutti

Laboratoire Louis Néel, B.P. 166 X, 38042 Grenoble Cedex, France

(*Reçu le 31 mars 1987, accepté le 19 juin 1987*)

Résumé. — Cette étude présente, à partir d'expériences et de simulations numériques, différents aspects des propriétés d'irréversibilité apparaissant dans les systèmes à anisotropie aléatoire à basse température. Les phénomènes d'hystérésis directionnelle et rotationnelle ont été particulièrement étudiés. Nous montrons en particulier que la distribution spatiale des directions de facile aimantation locale conduit à une distribution de coercitivité dans le système. L'évolution de l'aimantation lors de ces cycles d'hystérésis ou de couple magnétique se fait par une alternance de destruction et de reconstruction du moment total.

Abstract. — Starting from magnetization measurements and numerical simulations, this study shows different aspects of irreversible properties appearing in random anisotropy systems, at low temperature. Directional and rotational hysteresis phenomena have been particularly studied. As an example, we show that the spatial distribution of local easy directions of magnetization leads to a distribution of coercivity in the system. The evolution of the magnetization during these hysteresis loops is associated with an alternation of destruction and rebuilding of the total magnetic moment.

Introduction.

For about twenty years, random anisotropy systems usually called « amorphous ferromagnets » have been the object of many theoretical and experimental studies. On theoretical grounds, it seems now well admitted [1-5] that long range ferromagnetism is broken under the effect of a weak random anisotropy field. Experimentally, this conclusion is confirmed by different measurements on amorphous alloys with a relatively strong local anisotropy [6-9]. Moreover, different similarities with spin glasses have been observed around the phase transition and at low temperature [7-9]. However, it is still difficult to conclude in the case of low anisotropy systems because of the dominant role played by any parasitic coherent anisotropy, unavoidable in real samples.

This paper deals with some aspects of the irreversible properties which occur in the low temperature phase of these systems. The results presented here have been obtained on a rare earth based amorphous alloy : DyNi which presents a rather important local random anisotropy to exchange ratio ($D/J \approx 1$) [10].

In a first part, we present simple evidence for irreversibility in this system : the existence of thermal hysteresis between zero field cooled and field cooled experiments. The second and third parts deal respectively with uniaxial and rotational hysteresis loops obtained from magnetization and torque experiments. At each step, results of numerical simulations are presented which permit an understanding of the microscopic origin of the hysteresis of DyNi at low temperature.

1. Thermal hysteresis.

1.1 EXPERIMENTS : ROLE OF THE STRENGTH OF THE RANDOM ANISOTROPY. — In any magnetic system and particularly in disordered systems, a convenient way to see whether some irreversible phenomena occur at low temperature consists of measuring the thermal variation of the total magnetization $M(T)$ by increasing and then decreasing the temperature, the sample having previously been zero field cooled from the paramagnetic regime. This procedure has been intensively used for spin glasses and some results have been also published on the amorphous alloys $Dy_xGd_{1-x}Ni$ which are a realization of the random anisotropy axis model [7]. These previous results have shown that for each value of the applied

field, there exists a freezing temperature $T_F(H)$ above which the $M(T)$ variations are reversible and below which zero field and field cooled curves are different. The ratio $\frac{\Delta S}{S}$ of the surface delimited by these two curves to the surface delimited by the field cooled curve below $T_F(H)$ gives a rough measure of the importance of the irreversibility. In the series of amorphous alloys $Dy_xGd_{1-x}Ni$, it is clear that the irreversibility at low temperature increases with the random anisotropy to exchange ratio D/J (Fig. 1).

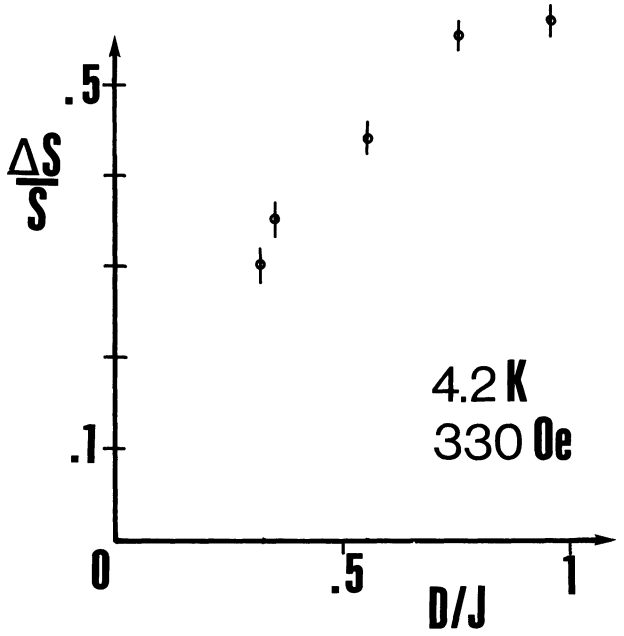

Fig. 1. — $\frac{\Delta S}{S}$ *vs.* D/J at $T = 4.2$ K and $H = 330$ Oe in the serie $Dy_xGd_{1-x}Ni$. For a more rigorous comparizon, the measures should have been made for the same $\frac{H}{T_t}$ and $\frac{T}{T_t}$ ratios ; this figure gives a qualitative feature of the increase of the irreversibility with D/J.

Moreover, the strength of the applied field has also a strong influence on the irreversibility because it reduces the pinning of the magnetization in metastable states. As shown in figure 2, a reduction of irreversibility under application of a magnetic field appears clearly together with a decreasing of the freezing temperature T_F. The field dependence of $T_F(H)$ is plotted in figure 3 ; for fields smaller than 250 Oe, it fits well the law $H = 2\,540$ Oe $(1 - T/13.5)^{1.55 \pm 0.05}$. This line represents in the (H, T) plane the onset of irreversibility of the longitudinal degrees of freedom which can be understood in spin glasses in terms of a crossover between weak and strong irreversibility [7, 11]. On the other hand, another crossover can be defined at lower temperatures. It is represented by the line $T_i(H)$ in figure 3 where $T_i(H)$ is the inflexion point of the zero field cooled curve. The equation of this line is

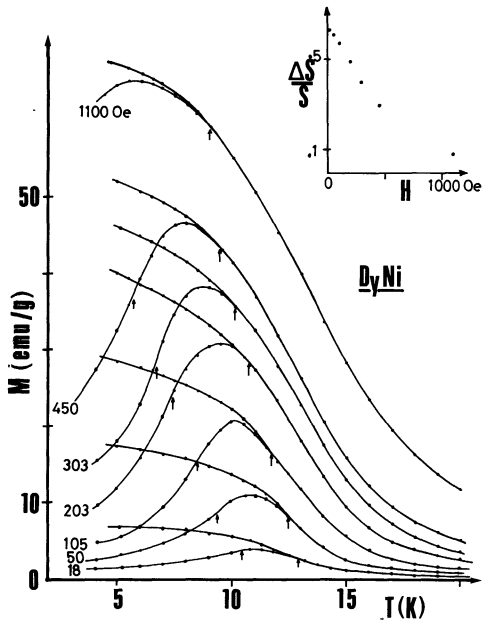

Fig. 2. — Zero-field and field cooled curves in DyNi for different values of the applied field. The arrows indicate $T_F(H)$ and $T_i(H)$. Insert : $\frac{\Delta S}{S}$ *vs.* H showing the decrease of the irreversibility with H.

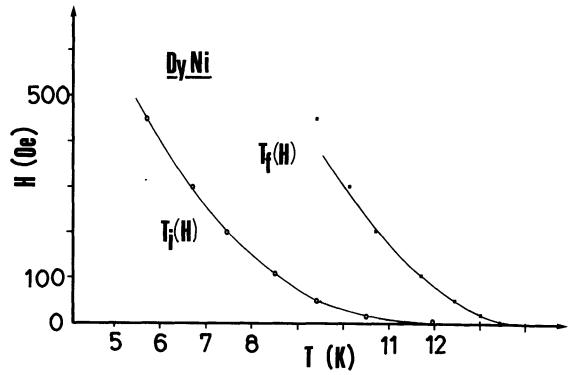

Fig. 3. — $T_F(H)$ and $T_i(H)$ lines. The solid lines are fits of the experimental points :

$$\frac{H}{2\,540 \text{ Oe}} = \left[\frac{13.5 - T_F(H)}{13.5}\right]^{1.55}$$

$$\frac{H}{2\,350 \text{ Oe}} = \left[\frac{12.5 - T_i(H)}{12.5}\right]^{2.7}.$$

phenomenologically given by $H = 2\,350$ Oe $(1 - T/12.5)^{2.7}$. The temperature $T_i(H)$ is the one for which the thermal activation becomes of the order of the average height of the energy barriers between metastable states. It corresponds also to the maximum rate of magnetic after-effect. So, the $T_i(H)$ line represents a crossover between a regime of strong pinning of the magnetization by random energy barriers due to the random anisotropy field to a regime of progressive depinning of the magneti-

zation by thermal activation. This crossover could also be defined by the inflexion point of the first magnetization curve for different temperatures and is also related to the line representing the thermal variation of the coercive field.

1.2 SIMULATION : MICROSCOPIC ORIGIN OF THE IRREVERSIBILITY. — Let us now look more precisely at the microscopic origin of this irreversibility at low temperature. For this purpose, we have made various simulations of three and two dimensional systems with an infinite random local anisotropy (Ising at each site). The easy axis of magnetization of site i being set by the randomly oriented unit vector $\hat{n}_i$, the atomic moment of site i has two possible states : $\mathbf{S}_i = \varepsilon_i \hat{n}_i$, $\varepsilon_i = \pm 1$. The Halmitonian of the system is $\mathcal{H} = \sum_{\langle i,j \rangle} J\hat{n}_i \cdot \hat{n}_j \varepsilon_i \varepsilon_j$ with $J > 0$ and $\langle i, j \rangle$ indicating all pairs of nearest neighbours. The procedure used consists of making an ultra fast cooling of the sample from a paramagnetic state down to 0 K. Figure 4a shows a typical example of a metastable state obtained at 0 K for a bidimensional sample of 100 × 100 spins. Several points are to be noticed :

i) The total energy of this metastable state, although higher than that obtained when the system has been slowly cooled, is lower than that obtained in any asperomagnetic state i.e. when all atomic moments point in the same hemisphere. This is an indication in favour of a breaking of ferromagnetism by the random anisotropy field.

ii) The positive exchange interactions tend to induce a local ferromagnetic order, but due to the randomness of the local anisotropy axis, magnetic moments lose rapidly their spatial coherence (beyond four or five atomic distances). Moreover, if the random anisotropy to exchange ratio D/J is reduced, the ferromagnetic local order tends to spread out, but beyond a characteristic length, depending on D/J, this ferromagnetism is broken.

iii) Although all exchange interactions are positive, some neighbouring moments are oriented in the opposite sense, i.e., there is some frustration in these systems as in spin-glasses but for different reasons. This frustration can be simply illustrated on a triangular lattice with infinite anisotropy along the three axis of the triangle (see Fig. 5).

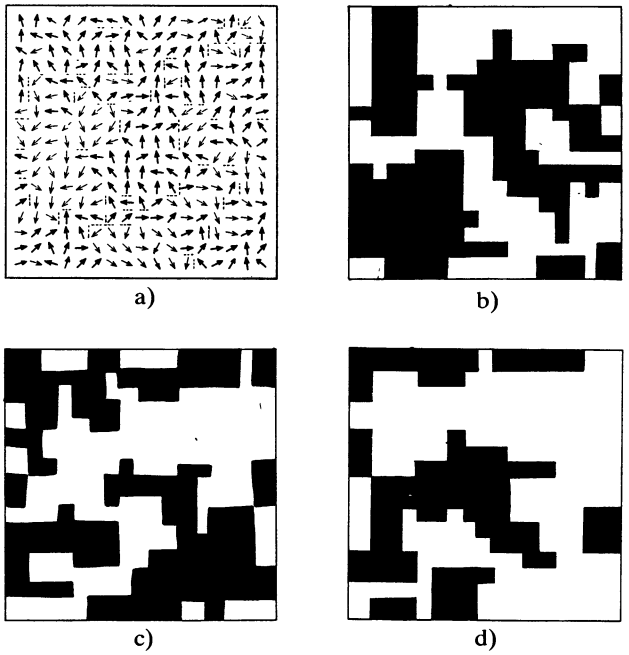

Fig. 4. — a) Part of a metastable state obtained at 0 K on a bidimensional sample of 100 × 100 spins. b), c), d) Three other metastable states of the same sample obtained for three different experiments. As only the sens of the spins can change from one state to another, we have only darkened the regions where the moments have been reversed in comparison to the reference state 4a.

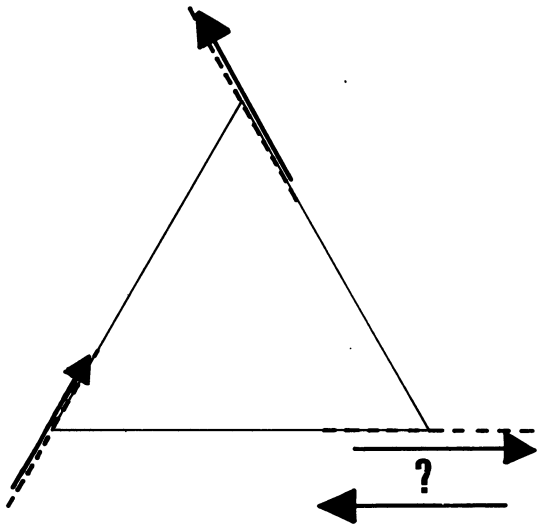

Fig. 5. — Frustration on a triangular lattice with infinite anisotropy along the three axes of the triangle. Although all exchange interactions are positive, there is always a pair of spins for which $\mathbf{S}_i \cdot \mathbf{S}_j < 0$.

iv) Figures 4b, c, d correspond to three other metastable states of the same sample obtained for three different experiments. As only the sense of the magnetic moment can change from one state to another, we have only darkened the regions on these figures where the moments have been reversed in comparison to the reference state (4a). The white regions correspond to the overlap between metastable states. From one state to another, it appears that the entities which reverse are not individual moments but blocks of moments of various sizes and shapes. This picture of the low temperature phase divided in such coherent blocks is similar to the one

proposed by Imry and Ma [1] in the case of ferromagnets with a random field. Moreover, the frontiers ot these blocks follow particular lines linked to the topological distribution of local anisotropy axis, particularly lines passing through those pairs of neighbouring sites having perpendicular easy axis of magnetization (these pairs correspond to a low effective exchange coupling).

In conclusion, this study of irreversibility in random anisotropy systems shows some similarities between these systems and spin-glasses at low temperature : frustration, metastability, irreversibility but, however, with an important increase of the initial susceptibility at low temperature in the present systems.

We present now some results concerning irreversible phenomena of the magnetic response under variations of an applied field.

2. Directional field hysteresis.

2.1 EXPERIMENTS. — First magnetization and hysteresis loop experiments have been performed on DyNi at various temperatures between 14 K and 1.5 K and for applied fields slowly varying from 0 to + 50 kOe and then from + 50 kOe to − 50 kOe at a constant rate of 2 Oe/s. In these experiments, the sample was initially zero field cooled from the paramagnetic regime ($T \gg 13.5$ K) down to the temperature of measurement.

First magnetization curves are presented in figure 6, hysteresis loops in figure 7. The inflexion points which can be seen at low temperature on first magnetization curves reflect the crossover, already mentioned, between a regime of pinning of the magnetization in metastable wells due to the random anisotropy to a progressive depinning due to the coupling to the applied field. This pinning is responsible for the difficulty in reaching the reversible part of the hysteresis loop at low temperature. Concerning the shape of the hysteresis loops, they are symmetrical and very strongly temperature dependent (due to the thermal activation mechanism and to the proximity of the phase transition occurring at

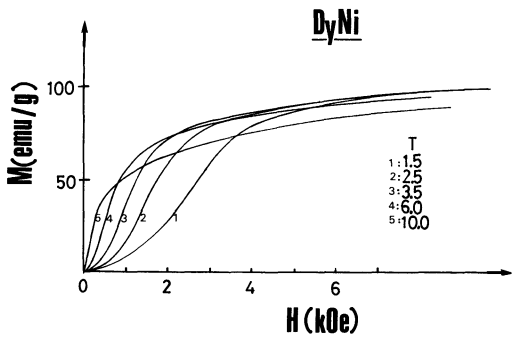

Fig. 6. — First magnetization curves in DyNi for different temperatures.

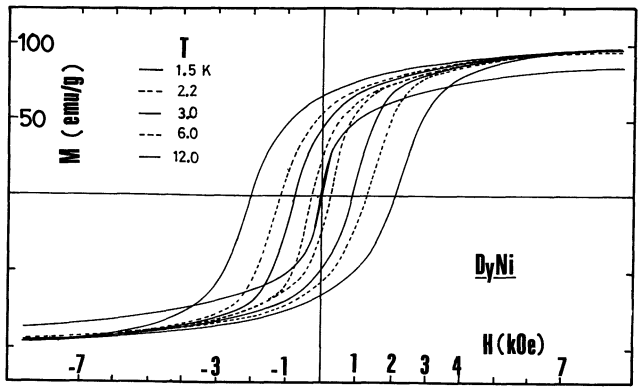

Fig. 7. — Hysteresis loops in DyNi for different temperatures.

$T_t = 13.5$ K [7]. Moreover, at intermediate temperatures (6 K $< T <$ 10.5 K) a very important after effect is observed near the coercive field. To characterize the effects of temperature, we have plotted in figure 8 the thermal variations of the coercive field together with the energy dissipated per cycle. Both curves have the same shape with a logarithmic part for intermediate temperatures (3 K $< T <$ 9 K) but steeper variations at low ($T <$ 3 K) and high (9 K $< T <$ 13.5 K) temperatures. For intermediate temperatures, $H_c(T)$ and $E(T)$ can be phenomenologically expressed by :

$$H_c(T) = 2.77 \text{ kOe} \times \exp(-T/2.70 \text{ K})$$
$$E(T) = 11.2 \times 10^5 \text{ erg/g} \times \exp(-T/2.07 \text{ K}) .$$

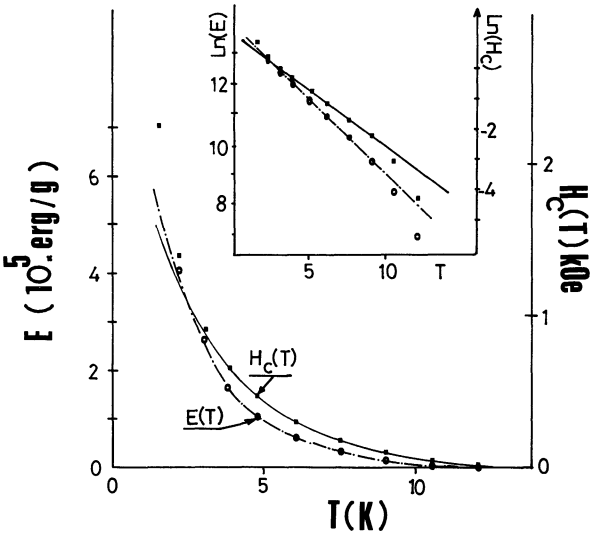

Fig. 8. — Thermal variation of the coercive field and of the energy dissipated per cycle. Solid lines are fits of respective equations :

$$H_c(T) = 2.77 \text{ kOe} \times \exp(-T/2.70 \text{ K})$$
$$E(T) = 11.2 \times 10^5 \text{ erg/g} \times \exp(-T/2.07 \text{ K}) .$$

Insert : same plot in semi-logarithmic scale.

Furthermore it is interesting to note that the remanent magnetization varies much slowly than the coercive field (Fig. 7).

2.2 SIMULATIONS. — We work at zero Kelvin on lattices of various sizes up to 60 × 60 at two dimensions and 15 × 15 × 15 at three dimensions. Periodic boundary conditions are applied and the magnetic moment and space dimensionalities are the same. The Hamiltonian is the one introduced by Harris, Plischke, Zuckermann [12].

$$\mathcal{H} = -D \sum_i (\hat{n}_i \cdot \mathbf{S}_i)^2 - J_0 \sum_{\langle i,j \rangle} \mathbf{S}_i \cdot \mathbf{S}_j - \mu_B \mathbf{H} \sum_i \mathbf{S}_i$$

where

$\hat{n}_i$ are unit vectors randomly oriented on each site i,

$\mathbf{S}_i$ representing the moment i,

$\mathbf{H}$ is the applied field,

D and J_0 are constants characteristic of the amplitude of the local uniaxial anisotropy energy and of the exchange energy at the atomic scale.

The three following parameters can be modified :

- Size of the sample.
- Random anisotropy to exchange ratio D/zJ_0, z : number of nearest neighbours.
- Applied field to exchange ratio : H/zJ_0.

In all cases, the ratio D/zJ_0 is chosen greater than or equal to 1 so that the size L of ferromagnetic like domains determined by Imry and Ma's criterion [1] : $L \sim \left(\frac{J}{D}\right)^{\frac{1}{2-d/2}}$ is always much smaller than half of the size of the sample. The used procedure is a Monte Carlo algorithm and the final relative precision of the total energy reached for each step of the applied field is 10^{-6}.

The results are very similar in two and three dimensions for the range of D/zJ_0 ratio greater than 1. Figure 9 shows the loop obtained in the condition of DyNi ($D/zJ_0 \approx 0.95$) on a 15 × 15 × 15 lattice together with the variations of the modulus of the total moment. Several points may be noted :

i) The shape of the calculated loop is more abrupt than the measured one and correlatively the coercive field obtained here : 47 kOe is about twenty times larger than the one expected experimentally in the limit of absolute zero temperature. These differences between experiments and simulations are often observed. They are mostly due to the fact that thermal activation phenomena and multimoment reversal processes are not taken into account in numerical simulations.

ii) Figure 9 shows a huge reduction of the modulus of the total moment near the coercive field. This clearly indicates that the microscopic mechanism of magnetization reversal is not a rigid rotation of the assembly of moments but a successive destruction and rebuilding of the magnetization. More precisely, the configurations of individual moments have been visualised for different values of the reverse field near the coercive field (Fig. 10a, b, c, d corresponding to 0.9 H_c, H_c, 1.1 H_c, 1.3 H_c) in the case of a 2D

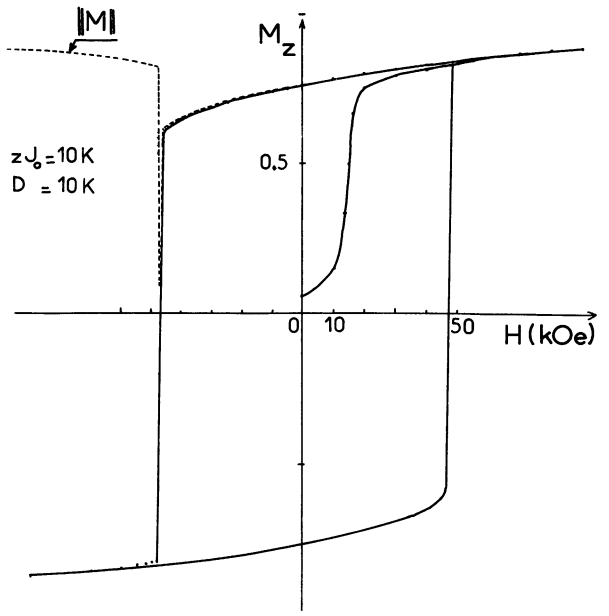

Fig. 9. — Calculated hysteresis loop obtained in the conditions of DyNi ($D/zJ_0 \approx 0.95$) on a 15 × 15 × 15 lattice. The dotted line represents the variations of the modulus of the total moment.

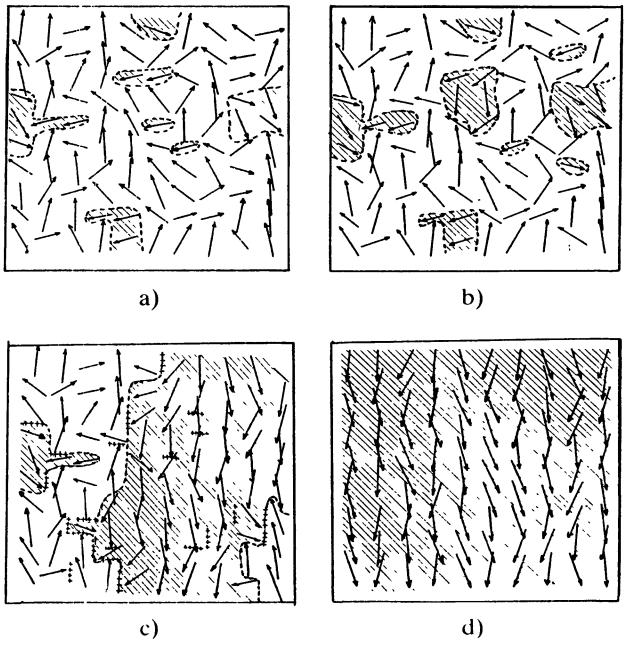

Fig. 10a, b, c, d. — Visualisation of the configurations of spins for different values of the reverse field near the coercive field (respectively H = 0.9 H_c, H_c, 1.1 H_c, 1.3 H_c) in the case of a bidimensional sample with D/zJ_0 = 1.

sample. Figure 10a shows that for $H = 0.9\ H_c$, some moments already point in the hemisphere of the field constituting nucleation centres for the reversal magnetization. These centres progressively take form and grow up (Fig. 10b). For $H = 1.1\ H_c$ (Fig. 10c), the sample is divided in two « domains » separated by a wall (area of high exchange energy). This wall follows some lines of lowest coupling, particularly by passing through pairs of neighbouring moments whose axis of easy magnetization are nearly perpendicular. Next, this wall propagates and sweeps through all the sample.

In conclusion, the microscopic process of magnetization reversal in rather high random anisotropy systems like DyNi is a « nucleation-propagation of walls » mechanism analogous to the one encountered in narrow wall ferromagnets [13] or Peierls systems.

For a given size of sample, this mechanism subsists as long as the random anisotropy to exchange ratio is not too small (the width of a wall must be much smaller than half of the size of the sample). For small D/J, a coherent rotation of all the magnetization is observed.

3. Rotational hysteresis : torque experiments.

3.1 EXPERIMENTAL RESULTS. — These experiments have been performed on a disc of DyNi of 30 μm thick with a new set-up in which the components M_X and M_Y of the magnetization are simultaneously measured during the rotation of the sample around the Z-axis (Fig. 11), the field being applied along the X axis. The sensitivity of 10^{-7} and 10^{-6} emu for respectively the X and Y components in a field of 10 Oe has been achieved by two SHE SQUID detectors.

Such an experiment brings much more informations than a conventional torque experiment since it allows the orientation and modulus of the total moment to be known at each step of the rotation and not only its M_Y component. The experimental procedure was the following.

i) The rotation being stopped, the sample is cooled from the paramagnetic region ($T \gg 14$ K) down to the measuring temperature in a saturating field of 20 kOe along the X-axis.

ii) Then, the saturating field is suppressed and we apply the measuring static field, generally much smaller than the saturating field.

iii) At $t = 0$, the rotation is started and the variations of M_X and M_Y are recorded. For the experiments presented here, the rotation speed is constant equal to 36 s per cycle.

iv) At the beginning, a transient regime is observed, the duration of which depends on the temperature and on the proximity of the measuring field to the coercive field. It can hold on up to 40 cycles before reaching the permanent regime. After the study of this permanent regime, we look on the influence of an inversion of the rotation direction.

Figure 12 presents raw results obtained from the two SQUID detectors for $T = 7.0$ K and a measuring field $H = 600$ Oe. When the permanent regime is reached, the M_X and M_Y components can be well represented as the sum of two contributions : a first one constant and the other with a periodicity of 2 π. A Fourier analysis of this periodic signal shows that the amplitudes of the different harmonics constitute less than 0.5 % of the fundamental measured in zero field and remains of the same absolute order of magnitude for the whole range of fields investigated. As a consequence, the magnetization can be considered as the sum of two contributions : the first one, $\mathbf{M}_1$, being weakly coupled to the sample

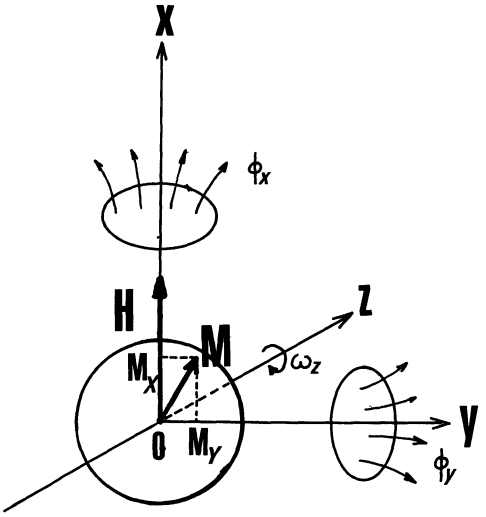

Fig. 11. — Principe of the set up used for the rotational hysteresis measurements.

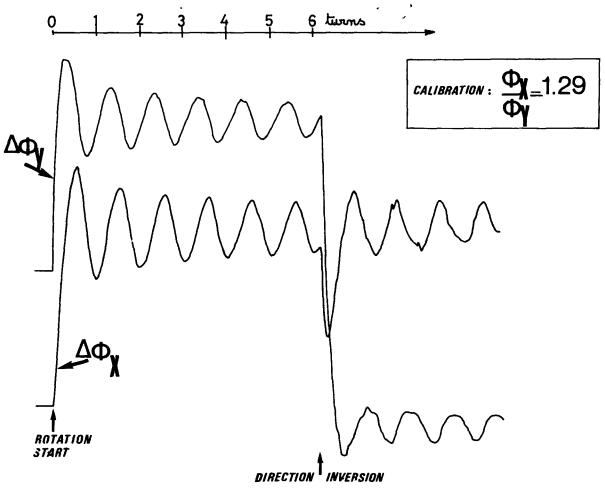

Fig. 12. — Raw results obtained from the two SQUID detectors for $T = 7.0$ K and measuring field H : 600 Oe.

remains fixed with respect to the applied field and the second one M_2, strongly bound to the sample through random anisotropy effects, is essentially fixed along the remanent magnetization induced before by the saturating field.

The evolution of these two contributions with the applied field are plotted in figures 13 and 14 for various temperatures. These evolutions result from the competition between the pinning effect of the remanent magnetization by the random anisotropy and the dragging effect of the applied field. For random anisotropy systems, a spatial distribution of coercivity exists principally due to the fluctuations of the distribution of local anisotropy axis but also depending of the history of the sample. The variations with the applied field of the magnetization fixed with respect to the sample can give a picture of this coercivity distribution. Indeed, for an increase ΔH of the applied field H, the increase ΔM of the pinned magnetization corresponds to the area of the sample the coercivity of which is between H and $H + \Delta H$. So the normalized derivative $\frac{dM_2}{dH}$ gives an idea of the coercivity distribution within the sample. These distributions are plotted for different temperatures in the insert of figure 14. It is worthwhile noticing that the maxima of these distributions corresponds well to the coercive field directly measured in the magnetization experiments (see Fig. 8), at least for temperatures greater then $\frac{T_t}{2} \approx 6.5$ K. For lower temperatures, the difference of characteristic time of the two experiments (500 s for the inversion of the field between + 500 Oe and − 500 Oe in the magnetization experiments and 18 s for a half turn in torque experiments) may explain the observed deviations.

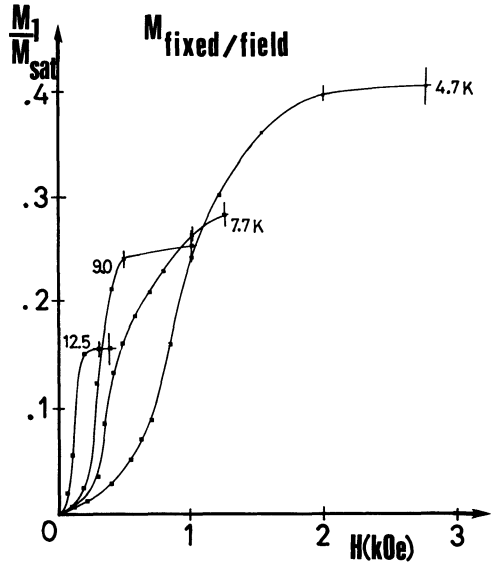

Fig. 13. — Variations with the applied field and for different temperatures, of the contribution to the magnetization which is weakly coupled to the sample and remains fixed with respect to the applied field (M_1).

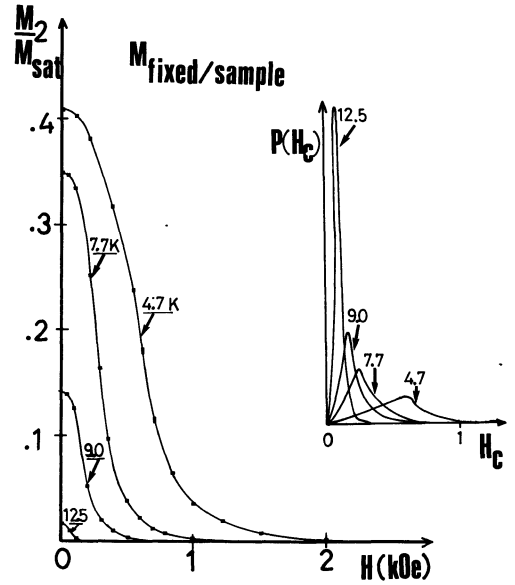

Fig. 14. — Variations with the applied and for different temperatures, of the contribution to the magnetization which remains strongly bound to the sample in the direction of the remanent magnetization (M_2). Insert : coercivity distributions defined by the normalized derivated $\frac{dM_2}{dH}$ for different temperatures.

The variations of the C_Z torque as measured by a conventional torque balance are simply obtained from the M_Y curves. This torque is again the sum of two contributions : a sinusoidal one (in first approximation) and a constant which reflects the dissipation in the system. They are both plotted in figure 15 for various temperatures. It is important to note that the presence of dissipation in this system with strong random local anisotropy can be seen in very high field (up to hundred times the coercive field). This

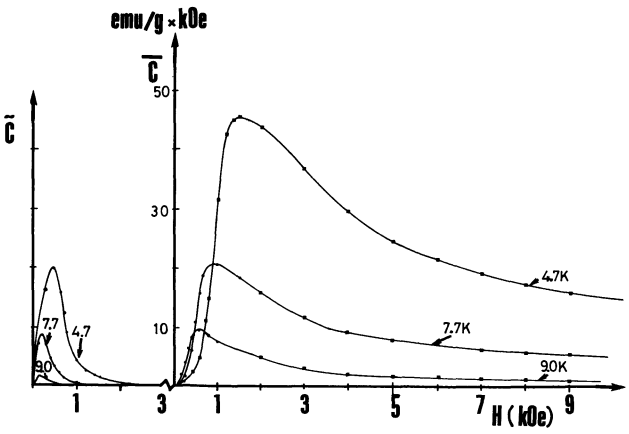

Fig. 15. — Variations with the applied field and for different temperatures, of the sinusoidal $\tilde{c}$ and constant $\bar{c}$ contributions to the C_Z torque.

constitutes an important difference with regard to the crystallised case with coherent anisotropy for which the dissipation disappears in twice or three times the coercive field.

3.2 SIMULATIONS. — As for the hysteresis loops, numerical have been performed together with the experiments in order to get more informations on the microscopic origin of the macroscopic observations. The numerical procedure performed for 2 and 3-dimensional samples is the same as the one used for the hysteresis loops. Typical results in the conditions of DyNi are presented in figures 16a and b for $H = H_c/2$. Due to the importance of the calculation time, only two turns of the sample have been calculated (exactly 640°) with a step of rotation of 10°. The following points are underlined :

i) The shape of the C_Z torque is in good agreement with the experimental results. It shows the beginning of transient regime and is essentially the sum of a constant torque and a sinusoidal one of periodicity 2π. We have verified for other conditions, that after a sufficient number of turns « quasi-permanent » regime is reached. This final regime is only « quasi-permanent » because of the metastability of the system at low temperature. Indeed, except for very low or very high applied fields, the path followed by the system in phase space is not exactly the same at each turn. These deviations bring relative fluctuations of the torque of the order of 5 % from one turn to another in the case of a $9 \times 9 \times 9$ sample.

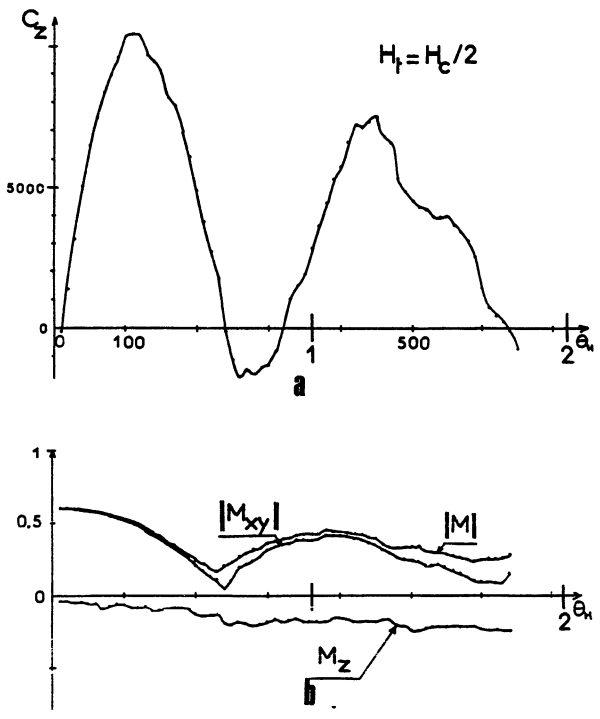

Fig. 16a et b. — Numerical simulations : a) Calculated torque C_Z *vs.* the angle of rotation of the field for $H_t = H_c/2$. b) Modulus of the total moment, of its projection M_{XY} in the plane of the turning field and of the perpendicular component M_Z *vs.* the angle of rotation of the field in the same run then 17a.

ii) The rotation of the total magnetic moment takes place with strong variations of its modulus (see Fig. 16b). Moreover, the result obtained for the variations of the modulus of the in-plane magnetization $\mathbf{M}_{XY}$ is in good agreement with the picture proposed in the previous paragraph : assuming that the magnetization $\mathbf{M}_{XY}$ is the sum of two contributions $\mathbf{M}_1$ and $\mathbf{M}_2$ of the same modulus for this value of the applied field, $\mathbf{M}_1$ being fixed with respect to the field and $\mathbf{M}_2$ fixed with respect to the sample, then $\|\mathbf{M}_{XY}\| = 2M|\cos\theta/2|$ where $\theta = (\mathbf{M}_1, \mathbf{M}_2)$. Such a form fits well with the results. Moreover, this picture has been confirmed by mapping the total projected moment $\mathbf{M}_{XY}$ for each step of the rotation. In particular, when $\|\mathbf{M}_{XY}\|$ becomes very small after a rotation of 240°, the sample is divided in two domains of opposite magnetization (projection in OXY) separated by a « wall » similar to that observed in the hysteresis loops at 2 or 3 dimensions in the vicinity of the coercive field.

iii) Moreover in three dimensional simulations, another phenomena occurs that cannot exist in 2 dimensions with XY moments : due to the considerable cost in exchange energy associated with the creation of a wall between domains of opposite in-plane magnetization, the system has rather created a Z-component in order to make the angle between the magnetization of each domains smaller and therefore to decrease the wall energy. This is the reason why an important increase of the M_Z component is observed during the rotation of the field (see Fig. 16b). Depending on the configuration of local axis of anisotropy, on the applied field and on the history of the sample, this M_Z component reaches a limiting value or changes sign periodically. This increase of M_Z leads to a decrease of the variations of the modulus of the total moment. For real samples, one can expect that this effect occurs only on a local scale with a compensation of positive and negative M_Z contributions at the macroscopic scale so that no macroscopic M_Z component arises. Clearly enough, for thin samples, these effects will be forbidden due to the demagnetizing field associated with the shape of the sample (non intrinsic).

iv) These phenomena (important variations of the modulus of the total moment and the arising of local M_Z component) exist only in the vicinity of the coercive field when the two types of domains (fixed or turning) coexist. In the other cases of very low or very high fields, the magnetization simply behaves like a single dipole :

— If $H \ll H_c$: this dipole corresponds to the

remanent magnetization initially created. It gives a 2 π periodic sinusoidal torque.

— If $H \gg H_c$: this dipole is nearly aligned with the applied field and feels all the distribution of random anisotropy axes. The obtained torque is sinusoidal, π periodic, not dissipative (see Fig. 17). The distribution of random anisotropy axes is then equivalent to an uniaxial resultant anisotropy. This is a statistic consequence of the finite number of elementary moments taken into account in the simulation. The strength of the resultant uniaxial anisotropy in high fields can be obtained by a random walk like treatment. It gives the size dependent effective anisotropy in $Dl^{d/2}$ that we effectively obtained by simulations at two or three dimensions. Unfortunately, such an effect cannot be seen in real samples ; coherent anisotropy phenomena (strains...), defects in the cutting of the disc... lead to much more important contributions which are probably responsible for the 0.5 % of harmonics previously mentioned in our experiments on DyNi.

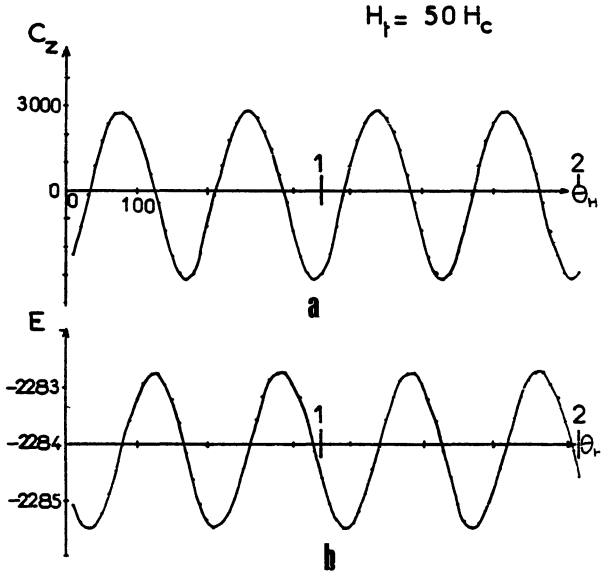

Fig. 17. — Numerical simulations : calculated torque C_Z and total energy E *vs.* the angle of rotation of the field for $H = 50\ H_c$.

Conclusion.

In conclusion, both hysteresis loops and torque experiments have shown that the topology of the local random anisotropy axis distribution plays an important role in these amorphous systems especially if the random anisotropy to exchange ratio is large. Indeed, this topology is responsible for the existence of lines of low energy coupling where the frustration generally localizes itself and which constitute initial centres in the « nucleation-propagation of walls » mechanism in the hysteresis loops or for the existence of a spatial distribution of coercivity which appears in torque experiments. As a consequence, the evolution of the magnetization under variations of the aplied field is achieved through strong variations of the total moment modulus for a wide range of fields around the coercive field. Moreover, in spite of the multitude of apparent intrinsic degrees of freedom, these variations can be described, in a schematic way, with a very small number of degrees of freedom.

In a follow-up to this study, it would be interesting to study the dynamical effects in these torque experiments, particularly the influence of the sample rotating velocity or the properties of rotational magnetic after effects in comparison with longitudinal after effects.

Acknowledgments.

We wish to thank J. P. Rebouillat and A. Lienard for sample preparation as well as P. Lethuillier, A. Barlet and J. C. Genna for help in magnetization measurements.

References

[1] IMRY, Y. and MA, S., *Phys. Rev. Lett.* **35** (1975) 1399.

[2] PELCOVITS, R. A., PYTTE, E. and RUSNICK, J., *Phys. Rev. Lett.* **40** (1978) 476.

[3] AHARONY, A. and PYTTE E., *Phys. Rev.* **B 27** (1983) 5872.

[4] CHUDNOVSKY, E. M. and SEROTA, R. A., *J. Phys.* **C 16** (1983) 4181.

[5] FEIGEL'MAN, M. V. and TSODYKS, M. V., preprint.

[6] VON MOLNAR, S., BARBARA, B, MC GUIRE, T. R. and GAMBINO, R. J., *J. Appl. Phys.* **53** (1982) 1350.

[7] DIENY, B. and BARBARA, B., *J. Physique* **46** (1985) 293 ; and *Phys. Rev. Lett.* **57** (1986) 1169 ; BARBARA, B. and DIENY, B., *Physica* **130B** (1985) 245 ; BARBARA, B., COUACH, M. and DIENY, B., *Europhys. Lett.* **3** (1987) 1129.

[8] HARRIS, A. B., CAFLISCH, R. G. and BARNAVAR, J. R., *Phys. Rev.* **B 35** (1987) 4929.

[9] SELLMEYER, D. J. and NAFFIS, *Phys. Rev. Lett.* **57** (1986) 1173.

[10] FILIPPI, J., DIENY, B. and BARBARA, B., *Solid State Commun.* **53** (1985) 523.

[11] MALOZEMOFF, A. P., BARNES, S. E. and BARBARA, B., *Phys. Rev. Lett.* **51** (1983) 1704.

[12] HARRIS, R., PLISCHKE, M. and ZUCKERMANN, M. J., *Phys. Rev. Lett.* **31** (1973) 160.

[13] BARBARA, B., *J. Phys.* **34** (1973) 1039.